EXPERIMENTAL AND NUMERICAL SIMULATION OF SINGLE-PHASE FLOW IN A MICRO HEAT SPREADER APPLIED TO THE COLD START OF INTERNAL COMBUSTION ENGINES FUELED WITH ETHANOL

Souza G.R.*, Moreira T.A., Vosnika A. and Ribatski G.
*Author for correspondence
Escola de Engenharia de São Carlos, Department of Mechanical Engineering,
University of São Paulo, São Carlos, SP, 400 Trabalhor Saocarlense Ave.,
Zip Code: 13560-970, Brazil,
E-mail: gustavor@sc.usp.br

ABSTRACT

This work presents the results of numerical simulations and experimental evaluation of a micro heat spreader applied to the cold start of internal combustion engines fuelled with ethanol. At low temperatures (below 11 °C), using only ethanol as fuel, engines are unable to start. So, it was adopted as solution in Brazil the use of gasoline to assist the first start. The gasoline is contained in an additional small reservoir implying on safety concerns. Additionally, the use of gasoline causes an increase of emissions compared with the use of only ethanol. Therefore, in the present study a micro heat spreader containing an electrical heater was developed in order to heat up the ethanol and permit the engine start under ambient temperatures down to -10 °C. Based on this, numerical simulations were performed using Computational Fluid Dynamics (CFD) software to predict the thermal behaviour of the device. Then, based on these simulations, a micro heat spreader was fabricated and experimentally evaluated. Good agreement between experimental and simulated results was obtained. Based on the initial results, the heat spreader seems to attend the requirements of its application.

INTRODUCTION

Otto cycle engines fuelled by ethanol have been presented as an alternative in a context of incentive to use renewable fuels. However, they still have some problems regarding cold start, problem aggravated in countries generally characterized by cold weather. It means by cold start the first start of the internal combustion engine after a period of 6 hours at least, which is in equilibrium at ambient temperature and the general temperature of the engine (parts, fluids, block, etc.).Some papers related to this work have been developed by other research centers, but under different conditions of temperature and positioning of the heat spreaders [1-7].

NOMENCLATURE

A	[m^2]	Area
a	[m]	Width
AF	[-]	Air-fuel ratio
b	[m]	Height
c	[kJ/kg K]	Specific heat
Co	[-]	Number of Courant
G	[kg/m²s]	Mass velocity
h	[W/m² °C]	Heat transfer coefficient
$\dot{m}$	[kg/s]	Mass flow
N	[rpm]	Engine speed
n	[-]	Constant (2 to 4-stroke and 1 for 2-stroke engines)
Nu	[-]	Nusselt number
P	[kPa]	Pressure
Q	[W]	Energy required
q	[W/m²]	Heat flux
ΔT	[°C]	Temperature difference between heat spreader output and input
$(\|U\|)$	[m/s]	Flow velocity
V	[m^3]	Volume

Special characters

α	[-]	Aspect ratio
λ	[-]	Air-fuel mixture
ρ	[kg/m^3]	Specific mass
δt	[s]	Time-step
δx	[m]	Length of each finite volume

Subscripts

a	Air
D	Displaced by the piston
f	Fuel
KC	Kays and Crawford correlation
out	Fluid out
p	Pressure
SL	Shah and London correlation
$stoic$	Stoichiometric
$surf$	Surface
$wall$	Wall

MATERIALS AND METHODS

Heat Spreaders based on Microchannels

A volume control analysis was conducted over the ethanol heating device for setting the temperature of the fuel injected near the intake valve in order to provide cold start of the internal combustion engine at -10 °C (ambient temperature), whereas the required temperature of air-fuel mixture in the intake manifold is 12 °C at 1 atm [8].

The mass flow of air ($\dot{m}_a$) and fuel ($\dot{m}_f$) were obtained based on the volume displaced by the piston (V_D = 0.001 m^3), the density of air at a temperature of - 10 ° C (ρ = 1.3378 kg/m^3), the starting rotation of the engine (N = 500 rpm) and n is 2 to 4-stroke and 1 for 2-stroke engines according to the following equation:

$$\dot{m}_a = \frac{V_D \rho N}{n\,60} \quad (1)$$

Assuming the stoichiometric air-fuel ratio, AF_{stoic}, of 9, from the molar balance of the combustion equation, and assuming at the time of cold start the air-fuel mixture as rich (λ = 0.9), the mass flow of fuel is given as follows:

$$\lambda = \frac{AF_{real}}{AF_{stoic}} \quad (2)$$

where:

$$AF_{real} = \frac{\dot{m}_a}{\dot{m}_f} \quad (3)$$

The vapor quality after the inlet manifold was considered for the air-fuel mixture equal to 0.1 and the temperature is 12 °C (temperature required after the inlet manifold to ensure ignition occurs, according to [8]), thus arrives at inlet fuel temperature control volume equal to 113.5 °C. Where $\dot{m}_a$ is 5.017 kg/h and $\dot{m}_f$ is 0.62 kg/h for each cylinder.

Based on this information, e the power supplied to the heat spreader in order of provide the energy required to heat up the ethanol to a temperature of 113.5 °C was obtained equal to 56 W. This power is provided by the electrical resistance illustrated in Fig. 1. Through the Laws of Conservation of Mass and Energy is obtained the power (W) provided by the resistance which is considered the total power required to raise the temperature of the fuel

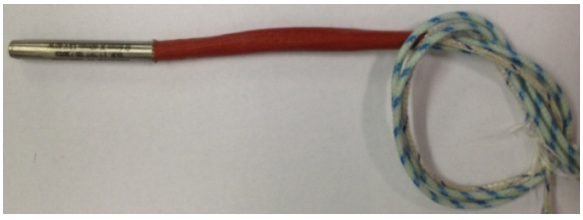

Figure 1 Electrical heater (6 mm x 40 mm, 12 V, 65 W).

The heat spreader illustrated in Fig. 2 consist of a brass cylinder with external diameter of 13 mm in which were machined 20 channels long 40 mm with cross sections areas of 0.5 x 1.73 mm². The electrical heater with a diameter of 6 mm is positioned internally to the heat spreader. The heat flux was defined as the ratio between the power supplied by the heater and the surface area of the heat spreader contacting the working fluid as follows:

$$q = \frac{W}{A_{surf}} \quad (6)$$

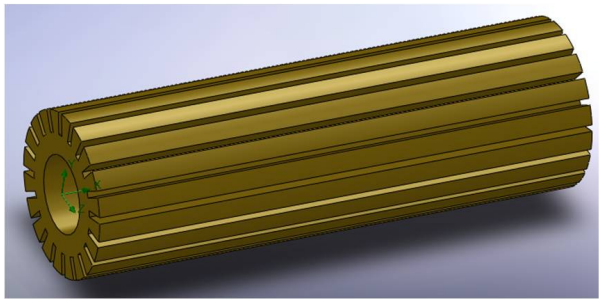

Figure 2 Design of the heat spreader made of brass.

Numerical Simulation

Numerical simulations of the flow were performed using OpenFOAM in order to analyze the results for pressure, temperature and speed. The transient solver solution was adopted that takes into account e the expansion and contraction of the fluid due to thermal effects. Based on the symmetry of the problem and neglecting fluid misdistribution due to gravitational effects, simulations were carried only for a single channel assuming uniform heat flux distribution and the mass flow thought a channel given by the ratio between the total mass flow rate and the number of channels.

A factor that determine the convergence and accuracy of the simulation is the number of Courant (Co) which relates the time-step (δt) and the length of each finite volume (δx), which depends on the resolution of mesh, with the module of the velocity flow ($|U|$).

$$Co = \frac{\delta t.|U|}{\delta x} \quad (7)$$

It is recommended that the maximum value of this variable is less than 1 during transient simulations. Values between 0 and 0.5 result in better accuracies in a longer processing time [9].

The mesh had 54000 hexaedric parts (27 x 10 x 200), remaining in this configuration during the simulations. As the mesh has a fixed resolution was defined that in the "control" of the solutions the time-step iteration should be variable, depending on the maximum magnitude of the flow velocity, so that the Courant number does not exceed the maximum 0.2, ensuring the convergence of the solutions.

Experimental set-up

The experimental tests were performed on a test facility, illustrated in Fig. 3, able of emulating conditions which are expected in case of the heating system is connected to the internal combustion engine (MCI).

Two thermal baths were used in order of obtaining ethanol temperatures at the heat spreader inlet -10 °C.

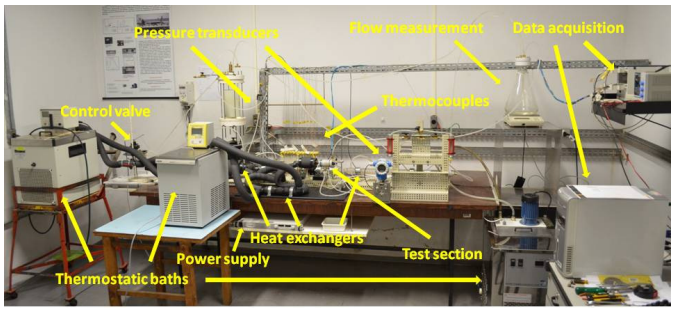

Figure 3 Experimental set-up.

Tests section

The test section is composed of PVDF flanges (heat insulating material which supports high temperatures), a glass tube, four threaded rods , thermocouples at the inlet and at the outlet section and also allocated in the heat spreader walls, *Viton* O-rings and connections for pressure taps (Fig. 4). The heat spreader was allocated inside a glass tube in order of allows flow visualizations.

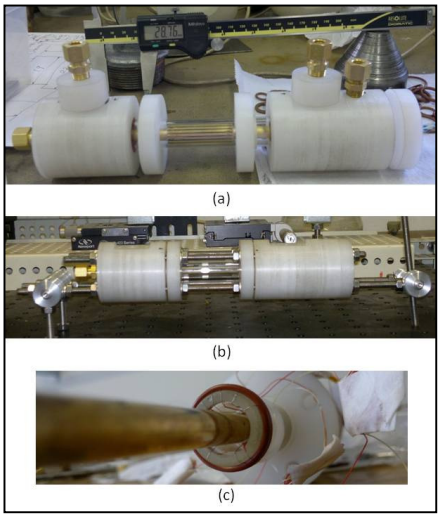

Figure 4 Assembly of the test section

As shown in Fig. 4, two shafts were connected to the heat spreader at its inlet and outlet sections. The first shaft has a conical shape in order of providing a better distribution of the liquid through the channels, the second one is used as tubing device for the cables of the thermocouples and electrical resistance. Electrical power is supplied to the electrical heater through a variable transformer, and the test section was covered by an isolation material to minimize heat losses.

Figure 5 shows the test section installed in the experimental setup. In this figure, it can also be observed the white *Nylon* flexible ducts connecting the test section to the inlet and outlet tubing and the pressure taps, the electrical resistance inserted into the heat spreader and it is for the cables that are connected to the power supply.

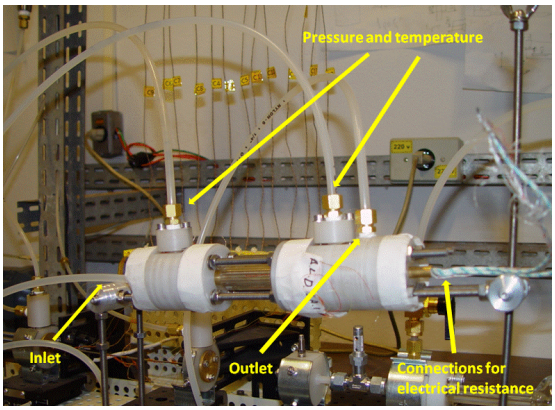

Figure 5 Test section.

Experimental uncertainty

Table 1 presents the experimental uncertainties of the measured and estimated parameters.

Table 1 Experimental Uncertainties

Parameters	*Uncertainty*
P	*4.5kPa*
G	*0.33 kg/m²s*
T	*0.15°C*
Q	*0.8%*

ANALYSIS OF THE RESULTS

The experimental results for the ethanol temperature at the outlet (T_{out}) of the heat spreader were compared also against theoretical values (Eqs. 8 and 9) obtained by the local heat transfer coefficient in the last section of the heat spreader:

$$Nu_{KC} = 8.235\left[1 - 1.883\frac{1}{\alpha} + 3.767\left(\frac{1}{\alpha}\right)^2 - 5.814\left(\frac{1}{\alpha}\right)^3 + 5.361\left(\frac{1}{\alpha}\right)^4 - 2\left(\frac{1}{\alpha}\right)^5\right] \quad (8)$$

$$Nu_{SL} = 8{,}235\left[1 - 2{,}0421\frac{1}{\alpha} + 3{,}0853\left(\frac{1}{\alpha}\right)^2 - 2{,}4765\left(\frac{1}{\alpha}\right)^3 + 1{,}0578\left(\frac{1}{\alpha}\right)^4 - 0{,}1861\left(\frac{1}{\alpha}\right)^5\right] \quad (9)$$

Where Nu_{KC} is Nusselt number by Kays and Crawford [10], Nu_{SL} is Nusselt number by Shah and London [11] correlations and α is aspect ratio of a single channel (b/a).

The theoretical temperature was estimated by the Newton´s Law of Cooling using the heat transfer coefficient calculated by Eqs. (8) and (9), as shown in the flowing equation:

$$\boldsymbol{T_{out} = T_{wall} - \frac{q}{h_t}} \quad (10)$$

Where q it is the heat flux transferred for the fluid estimated by an energy balance between the inlet and outlet of the test section.

Figure 6 illustrates the behaviour of the outlet temperature keeping a constant heat flux in the wall and varying the mass velocity. In both plots the trends of the calculated temperature and the experimental data measured during the experiments agrees reasonably well. It is important highlighting that the condition for the cold start of a internal combustion engine fuelled with ethanol occurs for low mass velocities corresponding in Fig. 6 to mass velocities around 10 kg/m^{2}s..

Based on the fact that the experimental apparatus was developed to perform experiments only at steady state conditions, numerical simulations (Figs. 7 and 8) were performed considering the preheating of the heat spreader and a non-constant mass flux, simulating a real engine start strategy.

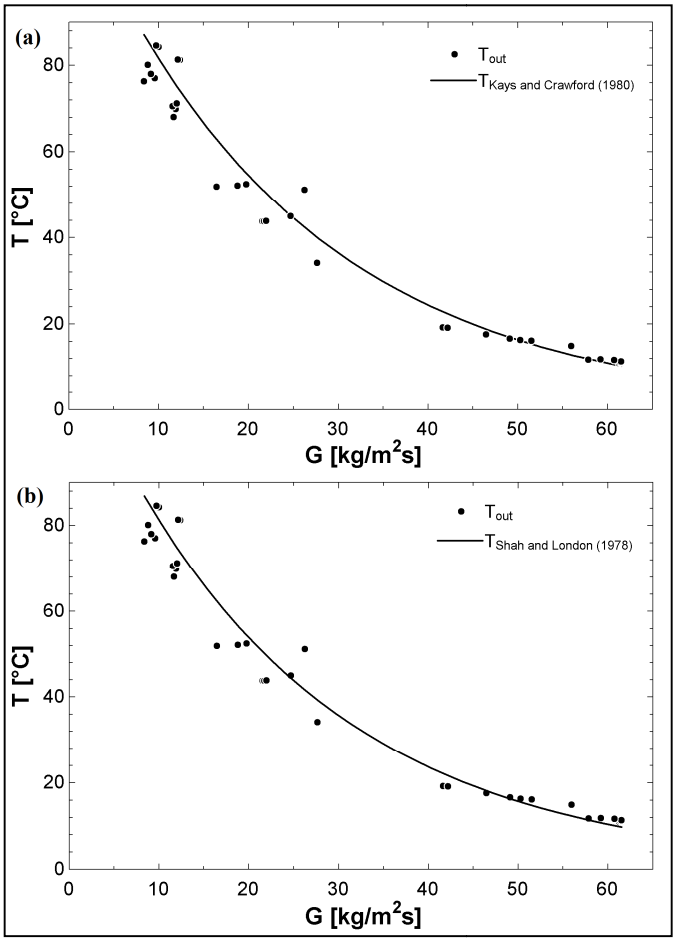

Figure 6 Comparison between the experimental data and the estimated values of outlet temperature of the ethanol by [10] (a) and [11] (b).

Figures 7 and 8 illustrate results of the transient variation of the ethanol temperature during the cold start. The simulations considered a heat flux of 15.74 kW/m², mass velocity equal to 10 kg/m²s and inlet temperature of -10°C.

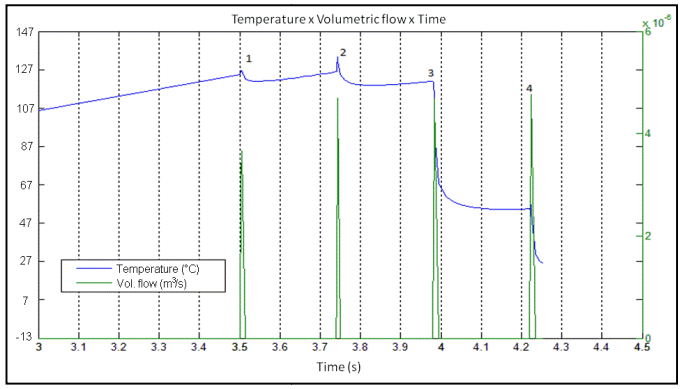

Figure 7 Outlet temperature (°C) vs. Volumetric flow (m³/s) vs. Time (s).

According to Figure 7, the ethanol is released in the initial two injections at high temperature, theoretically enough to achieve the minimum condition for the ignition of the fuel occurs efficiently in the combustion chamber. In the third injection, a parcel of the fluid is released at high temperatures and a portion at lower temperatures. From the 4th injection forward, the temperature that the fuel is sprayed into the collector is less than necessary as illustrated in Fig. 8.

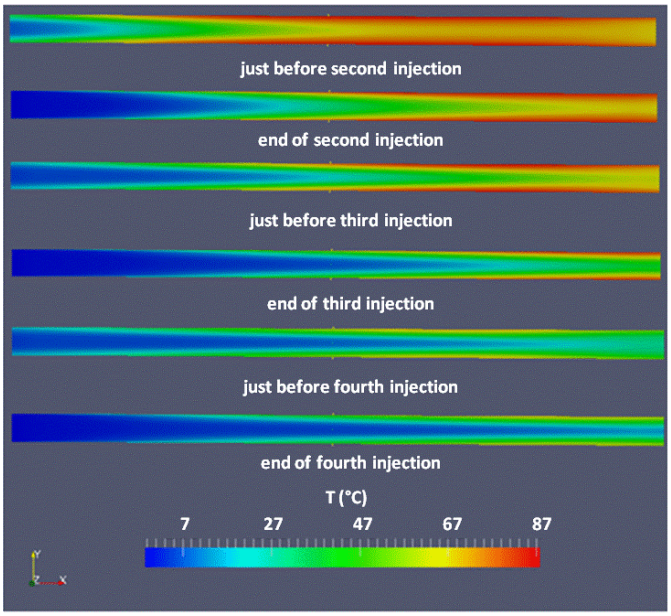

Figure 8 Temperature (°C) of the ethanol along the microchannel outlet at start and end of fuel injections.

Analyzing the results, it can be seen that the outlet temperature of the fluid in the first two injections is sufficient that the ethanol is ignited in the combustion chamber with a spark of the spark plug. The 3rd injection occurs at a temperature lower than the previous injections, but still with a high average of around 60 ºC. However the temperature at the 4th injection is much less than the necessary, with an average temperature below 40 °C.

CONCLUSION

The comparison between experimental data and correlations showed that the results obtained had a good behaviour with theoretical results. It is also concluded that the experimental apparatus presented a good agreement with the numerical simulations although the simulation considers a pre-heating of the heat spreader and did not consider the ambient losses. In the simulations it was observed that the first and second injections presented higher values of outlet temperature, due to the pre-heating of the heat spreader, which decreases in the next injections. For the next step will be performed experiments with the heat spreaders applied in an engine fuelled with ethanol, which will be kept in a cold chamber at -10°C.

ACKNOWLEDGEMENTS

The authors gratefully acknowledge the contribution of CAPES (Coordenação de Aperfeiçoamento de Pessoal de Nível Superior, Brazil) to the support of the Project Nº 059243/2010, and the scholarship Processes Nº #2013/02869-4, #2010/19944-0 and grant #2014/08449-0, São Paulo Research Foundation (FAPESP).

REFERENCES

[1] Kabasin, D., Hoyer, K., Kazour, J., Lamers, R. and Hurter, T. Heated Injectors for Ethanol Cold Starts. *Society of Automotive Engineers, Inc.* Paper SAE 2009-01-0615, 2009.

[2] Sales, L.C.M., Barbosa, R.F., Martins, L.A., Huebner, R., Santos, R.G. and Sodré, J.R. Numerical and experimental analysis of a cold start system used in flex fuel engines with heating of admission air and ethanol, *Society of Automotive Engineers, Inc.* Paper SAE 2009-36-0300, 2009.

[3] Short, J., Kazor, J.and Cavotta, M.; Thermal Modelling for Heated Tip Injectors, *Society of Automotive Engineers, Inc.* Paper SAE 2010-01-1264, 2010.

[4] Sales, L.C.M., Barbosa, R.F., Oliveira, F.M.V., Leal, W.F., Silva, Z.V. and Sodré, J.R. Heating system for ethanol and intake air - numerical model and experimental validation at cold start in a flex fuel vehicle with emissions analysis, *Society of Automotive Engineers, Inc.* Paper SAE 2010-36-0412, 2010.

[5] Colli, G.B., Castejon, D., Salvetti, A. and Volpato, O. Heated injector cold start system for flex-fuel motorcycles, *Society of Automotive Engineers, Inc.* Paper SAE 2010-36-0156, 2010.

[6] Sales, L. C. M. and Sodré, J. R. Cold start emissions of an ethanol-fuelled engine with heated intake air and fuel. *Fuel*, Vol. 95, 2012 pp. 122–125.

[7] Li, T., Deng, K., Peng, H. and Wu, C. Effect of partial-heating of the intake port on the mixture preparation and combustion of the first cranking cycle during the cold-start stage of port fuel injection engine. *Experimental Thermal and Fluid Science*, Vol. 49, 2013, pp. 14–21.

[8] Santos, A.M. Partida a frio de motores a álcool etílico com o auxílio do afogador. *VIII COBEM – Congresso Brasileiro de Engenharia Mecânica.* São José dos Campos - SP, pp. 245-248, 1985.

[9] OpenFOAM User's Guide. Disponível em 10/01/2014: <http://www.openfoam.org/docs/user/>.

[10] W.M. Kays, M.E. Crawford, Convective Heat and Mass Transfer, McGraw-Hill, New York, 1980.

[11] R.K. Shah, A.L. London, Laminar flow forced convection in ducts, Suppl. 1, Adv. Heat Transfer, 1978.